NWP SAF

Satellite Application Facility
for Numerical Weather Prediction

Document NWPSAF-KN-TR-006

Version 1.0

13-06-2008

SDP 2.0 validation

Jur Vogelzang

KNMI, De Bilt, The Netherlands

SDP 2.0 validation

Jur Vogelzang

KNMI, De Bilt, The Netherlands

This documentation was developed within the context of the EUMETSAT Satellite Application Facility on Numerical Weather Prediction (NWP SAF), under the Cooperation Agreement dated 16 December, 2003, between EUMETSAT and the Met Office, UK, by one or more partners within the NWP SAF. The partners in the NWP SAF are the Met Office, ECMWF, KNMI and Météo France.

Change record				
Version	Date	Author	Approved	Remarks
0.1	May 2008	Jur Vogelzang		First draft
0.2	May 2008	Jur Vogelzang		Added 100 km results
0.3	May 2008	Jur Vogelzang		Extended 100 km results
1.0	June 2008	Jur Vogelzang	Ad Stoffelen	Some comments

Contents

1 Introduction

1.1 Background

The SeaWinds Data Processor (SDP) generates ocean vector wind fields from the measurements of the SeaWinds scatterometer carried by QuikScat. SDP is a free software package developed in the framewotk of the Satellite Application Facility for Numerical weather prediction (NWP SAF) sponsored by EUMETSAT. A full description of SDP can be found in [*SCAT group*, 2007].

SDP 2.0 will replace SDP 1.5 medio 2008. The main differences between the two versions are:

- The default resolution of SDP 2.0 will be 25 km (was 100 km);
- The dimensions and cell size of the batch grid are now adjustable with the only restriction that they are even (they were fixed to dimension 32 × 32 points with a free edge of 5 points and a cell size of 100 km × 100 km);
- SDP 2.0 also processes the outer swath (wind vector cells 1-10 and 67-76);
- Improved rain flag handling.

From SDP 1.0 to 1.5, the following lessons were learned [*Vogelzang,* 2006, 2007]:

- At 25 km resolution, the Multiple Solution Scheme (MSS) must be used in order to suppress the noise in the retrieved wind fields, notably in the nadir swath;
- At 25 km resolution and with MSS, the Gross Error Probabilities should preferably be switched off.
- The free edge of 500 km (5 batch grid points) around the observations is rather small, since in the Tropics the background error correlation length equals 600 km.

Therefore these settings will be used as default by SDP 2.0.

1.2 Aims and scope

The possibility to change the batch grid size and dimension offers a whole range of new settings for 2DVAR. The optimum settings will be determined in this report. Further, the quality of the outer swath wind vectors will be assessed by statistical analysis of the differences with ECMWF background fields, rain flagging and MLE values, and a-priori probabilities.

Furthermore, the SDP wind product at 100 km is revisited, since NWP users require a more stringent quality control in the nadir swath, resembling the QC in the NOAA SeaWinds data from 2001-2007 (“old stream”).

1.3 Introductory remarks

Chapter 2 starts with some definitions and relations pertaining to the 2DVAR batch grid. This chapter is technical in nature, but may help in understanding chapter 3 where the optimum batch grid size and dimension are established by statistical analysis over one month of SeaWinds data obtained with various values for the 2DVAR batch grid parameters. The results for the outer swath at 25 km resolution are studied in chapter 4. This is also done in a statistical analysis: by comparing with model winds and by evaluating the properties of the rain flagging, MLE values, and a-priori probabilities as a function of Wind Vector Cell (WVC) number. The quality of the 100 km product is addressed in chapter 5. The conclusions can be found in chapter 6.

Appendix A contains a list of software used to produce the figures in this report. Appendix B contains a list of abbreviations and acronyms.

2 2DVAR batch grid

A complete description of 2DVAR is given in [*Vogelzang,* 2007], but in order to understand chapter 3, some basic definitions and relations pertaining to the 2DVAR batch grid will be given here.

The basic quantity is the batch grid size Δ. It can be set to 100000 m (100 km, default in SDP 1.5 and older), 50000 m (50 km), or 25000 m (25 km, default in SDP 2.0). Maybe a size of 12.5 km for ASCAT will be considered in the future; this is easily implemented in the code. The 2DVAR batch grid is a square grid, so its grid size is Δ in both directions.

The next important quantity is the observation sampling R. In SDP 2.0, R can have the same values as Δ, with the restriction $R \le \Delta$. If $R = \Delta$, all observations coincide with batch grid cells. If $R < \Delta$ the analysis is given on a coarser grid than the observations, so the analysis must be interpolated at some of the observation points. The number of wind vector cells (WVC's) per row is 19 for 100 km sampling, 38 for 50 km sampling, and 76 for 25 km sampling. The swath width S is 1900 km in each case.

Since the background part of the cost function is evaluated in the frequency domain rather than the spatial domain, the analysis increments on the 2DVAR batch grid must go to zero at the edges of the grid. Therefore a free edge is added around the batch grid. As a result, the observations are embedded in a larger grid. The size of the free edge is m grid points, so its spatial extension is $E = m\Delta$. This fixes N, the number of batch grid cells in the across track direction as

$$N = \frac{S + 2E}{\Delta} = \frac{S}{\Delta} + 2m \, . \qquad (1)$$

In the along track direction the part of the orbit being processed sizes T = 2200 km. The value of T is copied from SDP 1.5: with 32 batch grid points of 100 km in the along track direction and a free edge of 5 grid points there remain 22 grid points for observations. This fixes M, the number of batch grid cells in the along track direction as

$$M = \frac{T + 2E}{\Delta} = \frac{T}{\Delta} + 2m \, . \qquad (2)$$

Note that SDP 1.5 has Δ = 100 km and m = 5, so N should be equal to 29. Since the FFT algorithm in SDP 1.5 requires the number of batch grid cells in both directions to be a power of 2, N is set to 32. This means that on one side the number of free cells equals 8 rather than 5.

3 Batch grid size and dimension

3.1 Batch grid size

The first step is to determine the optimal batch grid size Δ. It has a default value of 100 km, but at 25 km resolution its value could also be 50 km or 25 km. All data from December 2004 were processed for Δ equal to 100 km, 50 km, and 25 km. The standard 2DVAR settings were applied, but without gross error probabilities and a free edge of 1800 km at least. Table 3.1 gives the 2DVAR batch grid parameters for these three runs. In some cases the dimension of the batch grid is slightly increased in order to avoid large prime factors in the FFT routine.

Run id.	Δ (km)	Batch grid dimension	Free edge (points)
D100_E1800	100	56 × 58	18
D050_E1800	50	112 × 120	36
D025_E1800	25	224 × 240	72

Table 3.1 Batch grid parameters.

The zonal and meridional wind speed components, u and v, were calculated for each wind vector cell (WVC) and the statistics of their differences were calculated by program DSW. The results are listed in table 3.2.

Grid size (km)		Zonal component *u* (m/s)				Meridional component *v* (m/s)			
Δ_1	Δ_2	bias	σ	min	max	bias	σ	min	max
100	50	+0.00071	0.38	-31.1	+24.2	+0.00003	0.35	-17.6	+22.7
100	25	+0.00074	0.38	-31.1	+21.6	-0.00018	0.35	-18.4	+22.7
50	25	+0.00004	0.096	-24.2	+15.3	-0.00021	0.096	-16.6	+13.5

Table 3.2 Statistics of the wind field comparison for various batch grid sizes.

Table 3.2 shows that the bias and the standard deviation σ are small, notably for the difference between the results with Δ=50 km and those with Δ=25 km, but that some large differences remain. The maximum differences in u between grid sizes of 100 km and 50 km occur for orbit 28552. Figure 3.1 shows the area of maximum difference in u. It lies in the Indian Ocean, east of Madagascar. WVC's rejected by the MLE flag are depicted in orange, those rejected by the VarQC flag in purple.

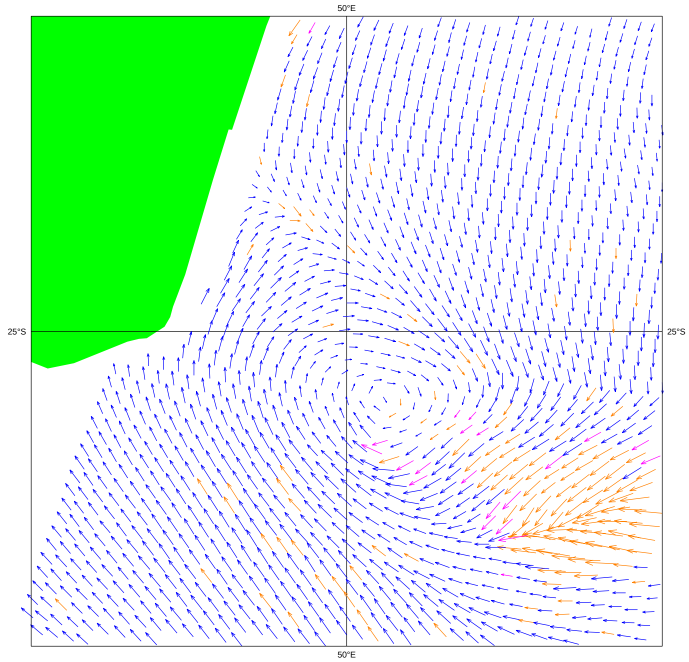
50°E
25°S
25°S
50°E

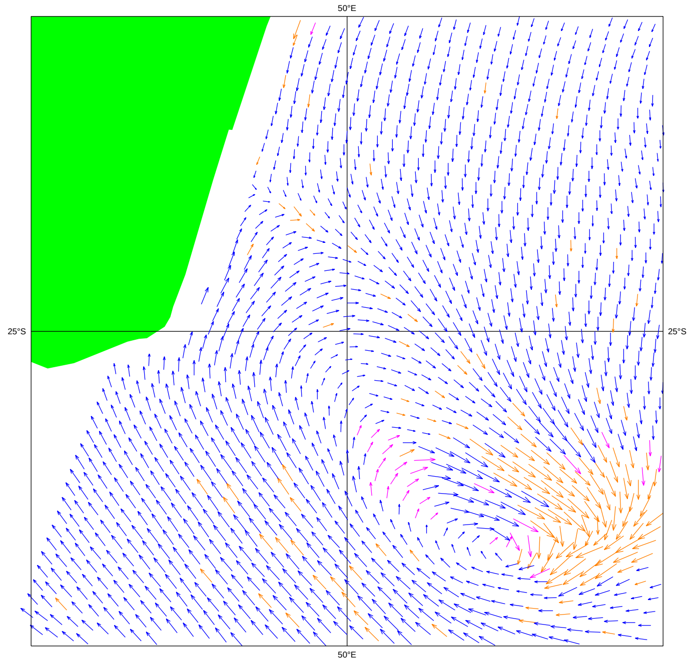
50°E
25°S
25°S
50°E

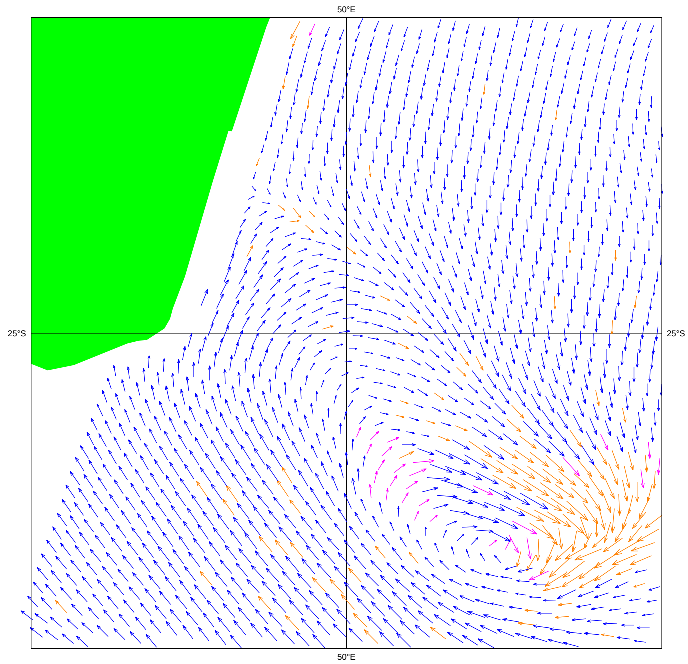

Figure 3.1 Wind field from orbit 28552 east of Madagascar with 2DVAR grid size of 100 km (upper), 50 km (middle), and 25 km (lower).

Figure 3.1 shows a large region with rain in the lower right corner. WVC's flagged with the rain flag do not contribute to the analysis, but do get a selected solution closest to the analysis. Since a large number of observations is missing, the analysis must be interpolated over a wide area, and small differences may lead to a different analysis and therefore to a different selected wind field. Further away from the rainy area the wind fields in figure 3.1 are the same.

Figure 3.2 shows the background field used in producing the wind fields of figure 3.1. The position of the low in figure 3.2 agrees well with the SDP results at 50 km and 25 km batch grid cell size. However, there are more cases like those of figures 3.1 and 3.2, and in some the SDP results with 100 km batch grid cell size are closer to the background. All these cases have in common that large patches are flagged by rain.

Note that the results obtained for Δ =25 km differ little from those for Δ =50 km. These results indicate that the optimum 2DVAR batch grid size is 50 km.

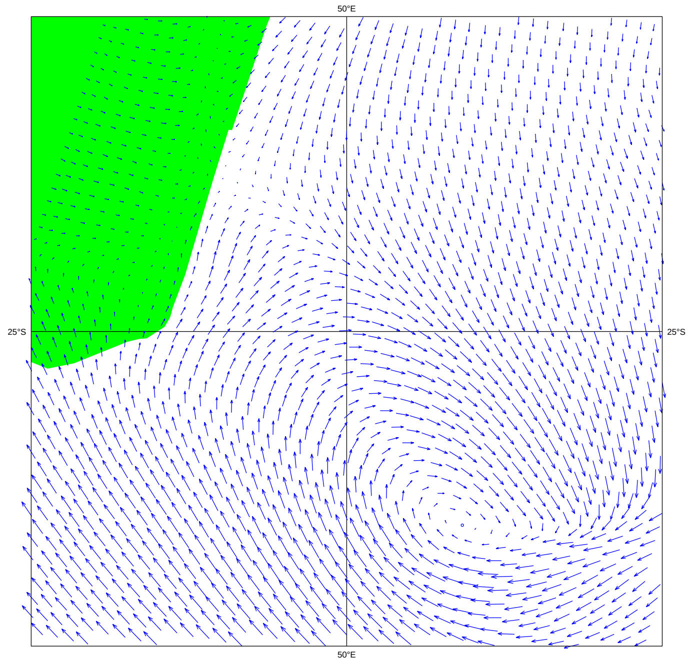

Figure 3.2 Background for the wind fields of figure 3.1

3.2 Batch grid free edge

In the previous section it was shown that the optimum batch grid size is 50 km. The next step is to determine the optimum size of E, the free edge around the 2DVAR batch grid. All data from December 2004 were processed for E equal to 1200 km, 1800 km, and 6000 km. The standard 2DVAR settings were applied, but without gross error probabilities. Table 3.3 gives the 2DVAR batch grid parameters for these three runs.

Run id.	*E* (km)	Batch grid dimension	Free edge (points)
D050_E1200	1200	88 × 92	24
D050_E1800	1800	112 × 120	36
D050_E6000	6000	280 × 288	120

Table 3.3 Batch grid parameters.

In some cases the dimension of the batch grid is slightly increased in order to avoid large prime factors in the FFT routine. The zonal and meridional wind speed components, u and v, were calculated for each wind vector cell (WVC) and the statistics of their differences were calculated by program DSW. The results are listed in table 3.4.

Free edge (km)		**Zonal component *u* (m/s)**				**Meridional component *v* (m/s)**			
		bias	σ	**min**	**max**	**bias**	σ	**min**	**max**
6000	1800	+0.00054	0.09	-14.0	+22.8	+0.00009	0.08	-13.4	+13.1
6000	1200	-0.00089	0.30	-26.5	+35.0	+0.00039	0.30	-21.4	+18.3
1800	1200	-0.00146	0.30	-26.5	+35.7	+0.00031	0.30	-21.4	+17.5

Table 3.4 Statistics of the wind field comparison for various free edge sizes.

Table 3.4 shows that the results for E equal to 1200 km differ from those for E equal to 1800 km or 6000 km, while the results for E equal to 1800 km resemble those for E equal to 6000 km. This indicates that the optimum value for the free edge size E is 1800 km.

The maximum difference found is in u between free edge size 1200 km and free edge size 1800 or 6000 km. This occurs for orbit 28525 in the northeastern Pacific. Figure 3.3 shows the wind fields in this region for the three free edge sizes. Figure 3.4 shows the NCEP background.

As in the previous section, the difference originates from an area with much rain where valid wind observations are sparse. The background field shows a front without very much structure. Northeast of the frontal zone the circulation direction is to the North. The SDP result with 1200 km free edge size shows an almost rotational structure in the frontal area, with a northwestern circulation right after the front. Note the abundance of VQC flagged WVC's (purple arrows) around the centre of the rotational structure.

The SDP results with free edge sizes 1800 km and 6000 km resemble each other. Here the frontal zone has disappeared and the change in wind direction extends over a larger area. Moreover, there are less VQC flagged WVC's. This indicates that the results with free edge sizes 1800 km and 6000 km are more reliable than those with free edge size 1200 km. From the point of computational efficiency, a free edge size of 1800 km is to be preferred.

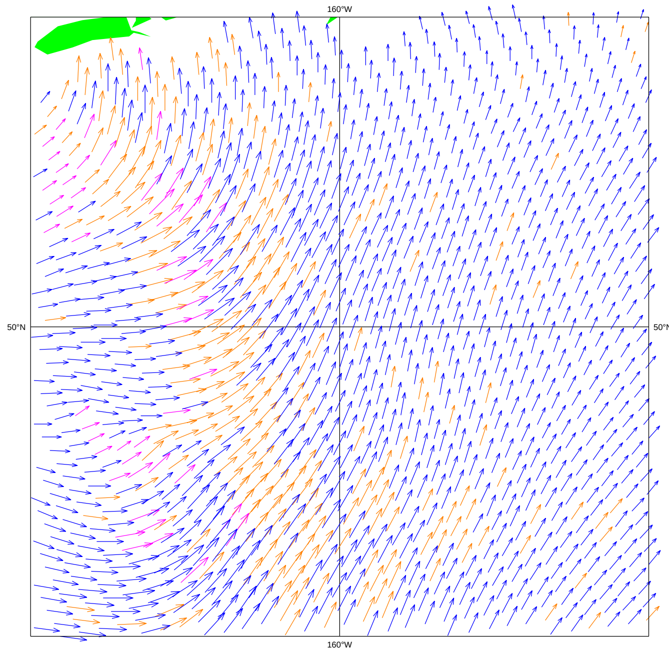

160°W
50°N
50°N
160°W

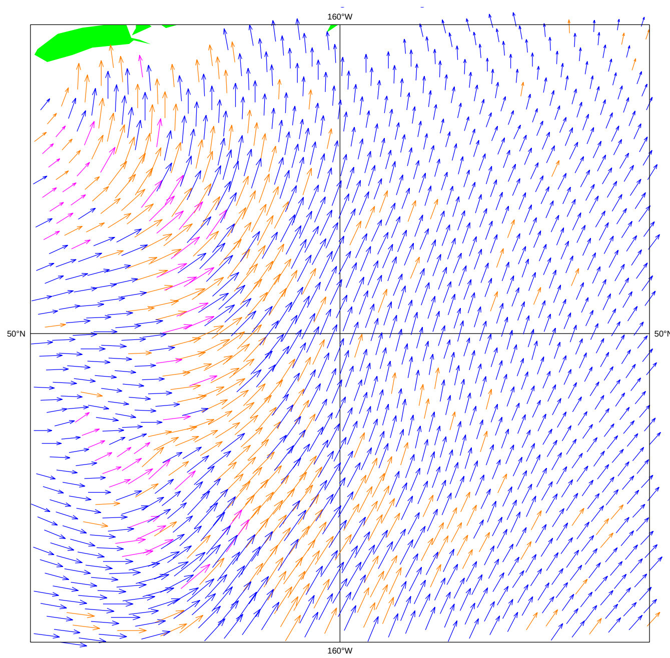

160°W
50°N
50°N
160°W

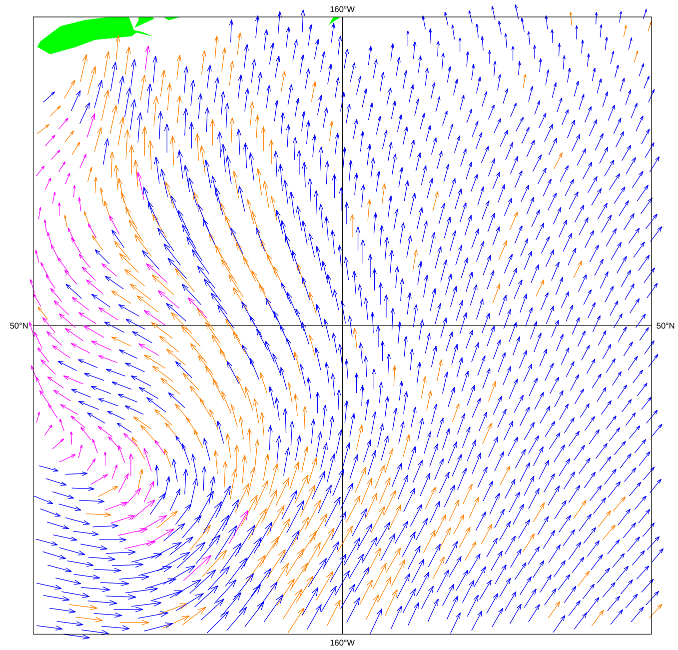

Figure 3.3 Wind field from orbit 28525 in the northeastern Pacific with 2DVAR free edge size 6000 km (upper), 1800 km (middle), and 1200 km (lower).

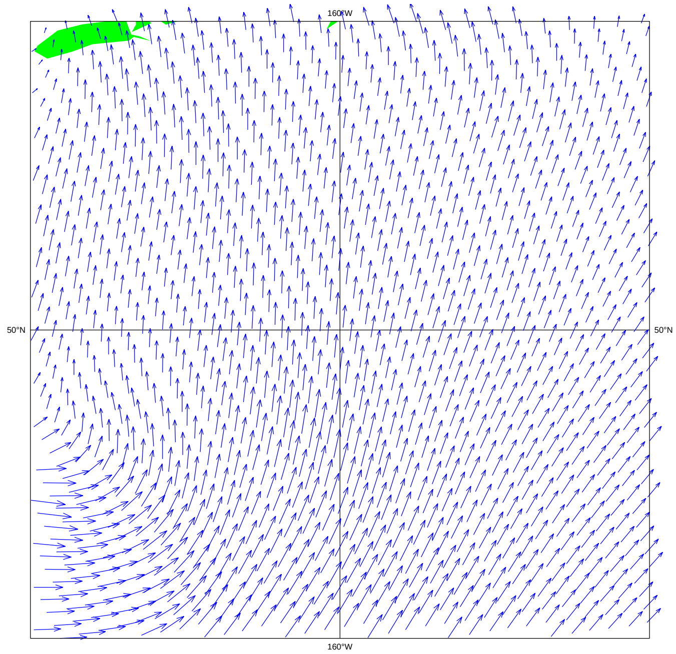

Figure 3.4 Background for the wind fields of figure 3.3.

4 Validation at 25 km resolution

4.1 Comparison with model winds

Now the optimum batch grid size and dimension have been established, the quality of the outer swath winds will be investigated. This is done for all SeaWinds data in the new NOAA format recorded in January 2008. The data were processed with SDP version 2.0 using the NCEP winds as background.

Figure 4.1 shows the standard deviation of the difference between the SDP selected wind and the ECMWF model prediction for the zonal wind component u and the meridional component v as a function of WVC number. Results are shown with MSS (black curves) and without (red curves). WVC's with the Cell Quality Flag or the Variational Quality Control flag set were excluded from figure 4.1. There are no selections in WVC 1 and WVC 76, so the standard deviation has been set to zero for these points.

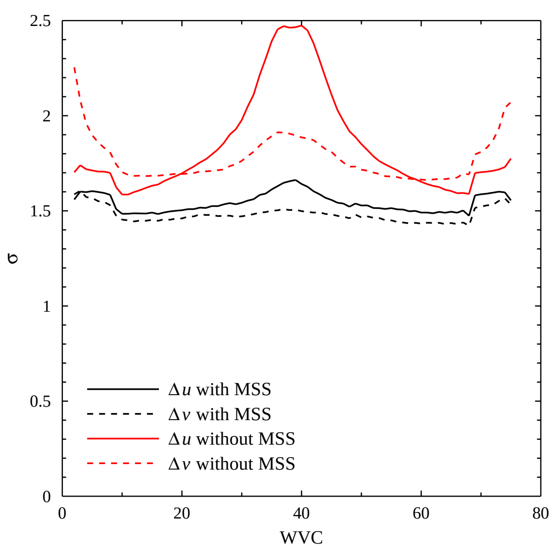

Figure 4.1 Standard deviation of the difference between the SDP selected winds with NCEP background and the ECMWF prediction as a function of WVC number for the components u and v.

Figure 4.1 shows that with MSS the standard deviation lies around 1.5 m/s, and that there is a weak dependency on WVC number: for the outer swath and the nadir swath the standard deviation is slightly larger than for the sweet swath. Without MSS the standard deviations are larger, especially for *u* in the nadir swath and for *v* in the outer swath. This is caused by the unfavorable measurement geometry in the nadir and outer swaths.

4.2 Rain flagging and MLE

From the data of January 2008 also the setting frequency of the KNMI-MLE bit in the cell quality flag (CQF) is extracted as a function of WVC number. The results are shown in figure 4.2.

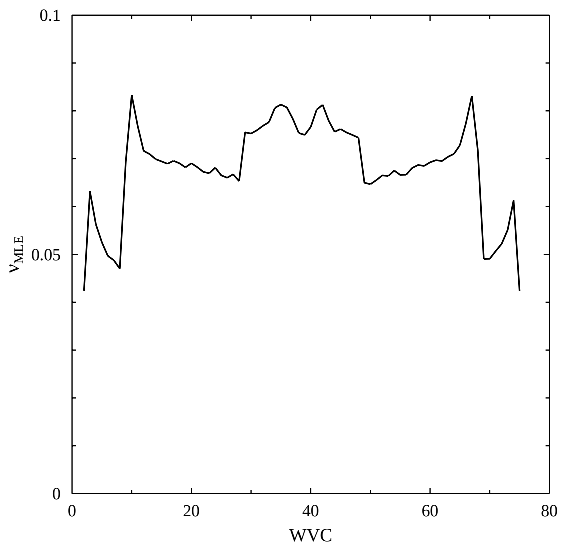

Figure 4.2 Frequency of setting the KNMI-MLE bit in the CQF as a function of WVC number.

The frequency of the rain flag setting is around 8% in the nadir swath and drops to about 7% in the sweet swath. At the end of the sweet swath, towards the outer swath, the frequency increases to more than 8%, but then drops sharply to around 5% in the outer swath. Since there are no wind selections in WVC 1 and WVC 76, the frequency is set to zero at these points.

The cell quality control procedure in SDP 2.0 for the outer swath is the same as that of the nadir swath: the KNMI-MLE bit in the CQF flag is set if the JPL rain bit in the original NOAA data is set or if the MLE exceeds a certain boundary. In the sweet swath the JPL rain flag is neglected. Apparently, this procedure accepts too much WVC's in the outer swath. Activation of the JPL bit yields only a small increase in the setting frequency of the KNMI-MLE bit in the CQF.

Figure 4.3 shows the average MLE value and its standard deviation for the solution selected by 2DVAR as a function of WVC number, excluding the WVC's that had the KNMI-MLE bit or the variational quality control (VarQC) bit set in the CQF. Both the average MLE and its standard deviation peak at the outer edges of the sweet swath (WVC 10 and 67). They decrease towards the nadir swath and the outer swath. Note the sharp decrease in σ for WVC 9 and WVC 69. These WVC's are at the very edge of the sweet swath and contain about half the number of valid cells compared to their direct neighbors.

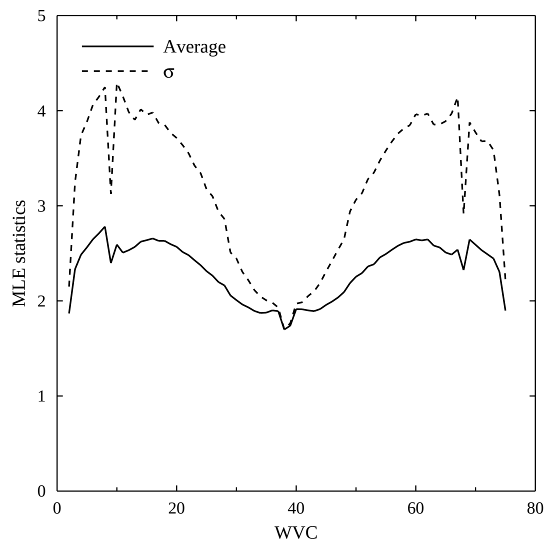

Figure 4.3 Average MLE (solid curve) and its standard deviation (dashed curve) of the 2DVAR solutions as a function of WVC number.

Figure 4.4 shows the normalized histograms of the MLE distribution of the 2DVAR solutions for WVC 2 (extreme outer swath), 10 (sweet swath), and 38 (central nadir), also obtained with program SBA. In the sweet swath there are less ambiguities with low MLE and more with high MLE compared to the outer and nadir swaths.

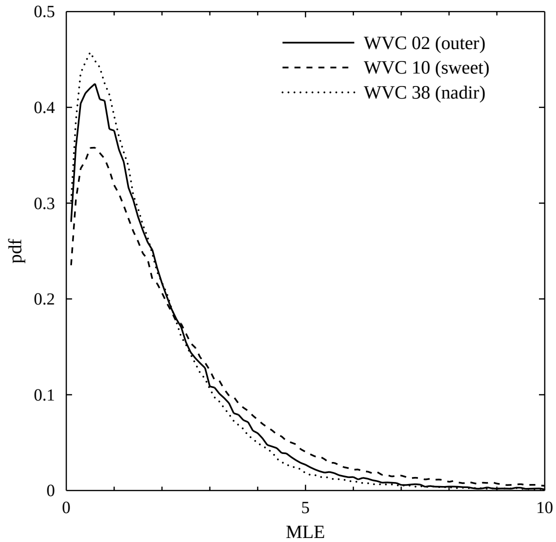

Figure 4.4 Normalized histograms for the MLE values at WVC's 2, 10, and 38.

The effects are less pronounced than in figure 4.3, because the mean and (especially) the standard deviation are sensitive to occasional high MLE values. Though WVC's with the KNMI-MLE bit or the VarQC bit set in the CQF were discarded, the maximum MLE value found can still be very high: 223.9 in WVC 67. The minimum MLE value found is zero for each WVC.

4.3 Probabilities

Figure 4.5 shows the 1st rank skills of 2DVAR and closest-to-background as a function of WVC number. The first rank skill of an ambiguity removal method is the frequency with which the method chooses the solution with highest a-priori probability. If the a-priori probability would have no effect on 2DVAR, the 1st rank skill would equal $1/144 \approx 0.007$. As can be seen from figure 4.5, it is significantly higher all over the swath, ranging from 0.03 at the outer swath and the nadir swath to more than 0.11 in the sweet swath. The first rank skill of closest-to-background is smaller than that of 2DVAR, because closest-to-background, unlike 2DVAR, does not take the a-priori probability into account. Nevertheless, the first rank skill of closest-to-background lies significantly higher than 0.07. his indicates that there are many WVC's for which the most likely scatterometer wind vector agree with the background.

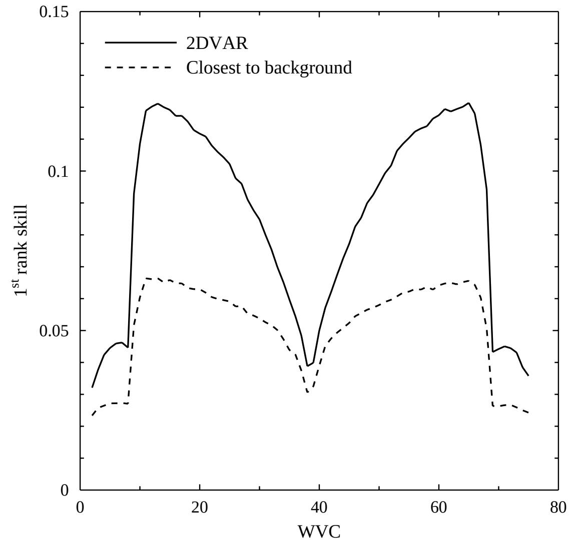

Figure 4.5 First Rank Skill of 2DVAR and closest-to-background versus WVC number.

Figure 4.6 shows some statistics of the probability of the solution selected by three ambiguity removal methods: First Rank (dotted), Closest-to-Background (dashed), and 2DVAR (solid). Figure 4.6 shows the average of the probability (black curves) and its standard deviation (red curves) as a function of WVC number. The curves are very similar: the highest values for average and standard deviation are obtained at the outer edge of the sweet swath while the lowest values are obtained in the central nadir and outer swaths. The highest average probability is found for the First Rank method. This is no surprise, because it selects the solution with highest probability by definition. The lowest average probability is found for the Closest-to-Background method, which does not take probability into account but only considers spatial consistency. The results for 2DVAR are in between as expected, because 2DVAR takes both the a-priori probability and spatial consistency into account.

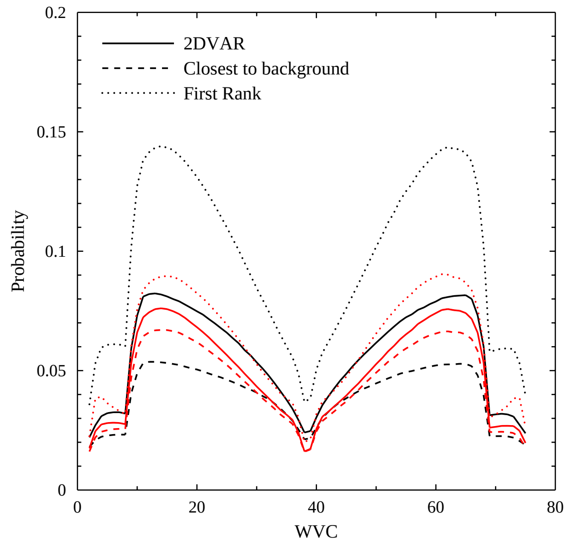

Figure 4.5 Average (black) and standard deviation (red) of the a-priori probability of the solution selected by 2DVAR (solid), Closest-to-Background (dashed), and First Rank (dotted).

5 Validation at 100 km resolution

The quality of the 100 km product is revisited after user requests, mainly pertaining to the nadir part of the swath. To this end, all SeaWinds data of January 2008 were processed with SDP version 2.0 at a resolution of 100 km using the NCEP winds as background. The size of the batch grid is 100 km, of course, while the free edge measures 1800 km as found in chapter 3 for 25 km resolution. This leads to a batch grid size of 56 points across track by 58 points across. The outer swath was included in the processing. In addition to the KNMI MLE QC [*Portabella and Stoffelen*,], the KNMI MLE flag was set in the outer swath if the JPL rain flag was set.

In an earlier study [*Vogelzang,* 2006] it was shown that SeaWinds data at 25 km resolution should be processed with MSS in order to suppress the observational noise, but that the noise is averaged out at 100 km resolution. Table 5.1 shows the standard deviation of the difference between the SDP wind components, *u* and *v*, and the ECMWF wind components. The values in table 1.5 are averaged over all nodes.

	σ_u (m/s)	σ_v (m/s)
No MSS	1.56	1.50
MSS	1.33	1.30

Table 5.1 Standard deviations between the SDP result at 100 km and the ECMWF model winds with and without MSS.

Table 5.1 shows that without MSS the standard deviation between the SDP result (obtained with NCEP background) and the ECMWF model is about 1.5 m/s for both components without MSS and drops significantly to 1.3 m/s when MSS is applied.

Figure 5.1 shows the standard deviations of the difference between the SDP results and the ECMWF model as a function of WVC. Without MSS the difference in *u* is up to 2 m/s in the nadir part of the swath. Application of the MSS reduces the difference to 1.4 m/s. This shows that the user's request may be fulfilled by applying MSS since MSS appears quite beneficial in the SDP 100 km product when verified with ECMWF.

Figure 5.1 shows the standard deviation of the difference in u and v between the ECMWF model and the SDP wind with or without MSS as a function of WVC number. Application of MSS decreases the standard deviation of the difference. The decrease is large in the nadir and outer swath, but still noticeable in the sweet swath. Figure 5.1 is similar to figure 4.1. Comparison of the two figures shows that the 100 km SDP product with MSS compares better to the ECMWF wind field than the corresponding 25 km product. Since 2DVAR in combination with MSS removes the observational noise from the 25 km SDP product, this difference must be due to small-scale features present in the SDP 25 km product but absent in the ECMWF model. In the 100 km SDP product, these small-scale features are averaged out and the comparison with the rather smooth ECMWF model is better.

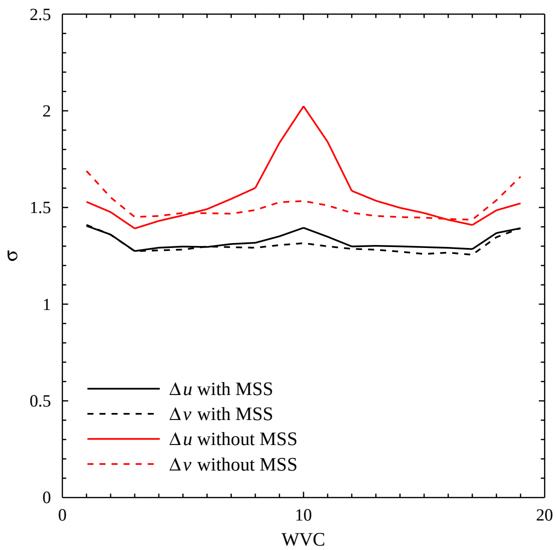

Figure 5.1 Standard deviation of the difference between SDP selected winds with NCEP background and the ECMWF prediction as a function of WVC number for the components *u* and *v* at 100 km resolution.

To check if the reduction in the standard deviation of the differences is indeed due to noise reduction by MSS and not to smoothing by increased background influence, figure 5.2 shows the autocorrelations in the wind components u (left hand panels) and v (right hand panels) for the outer swath, WVC 1 (top panels), the sweet swath, WVC 3 (middle panels), and the nadir swath, WVC 10 (lower panels). Each panel shows the autocorrelation of the ECMWF model (solid curves), the SDP selection without MSS (dashed curves), and the SDP selection with MSS (dotted curves).

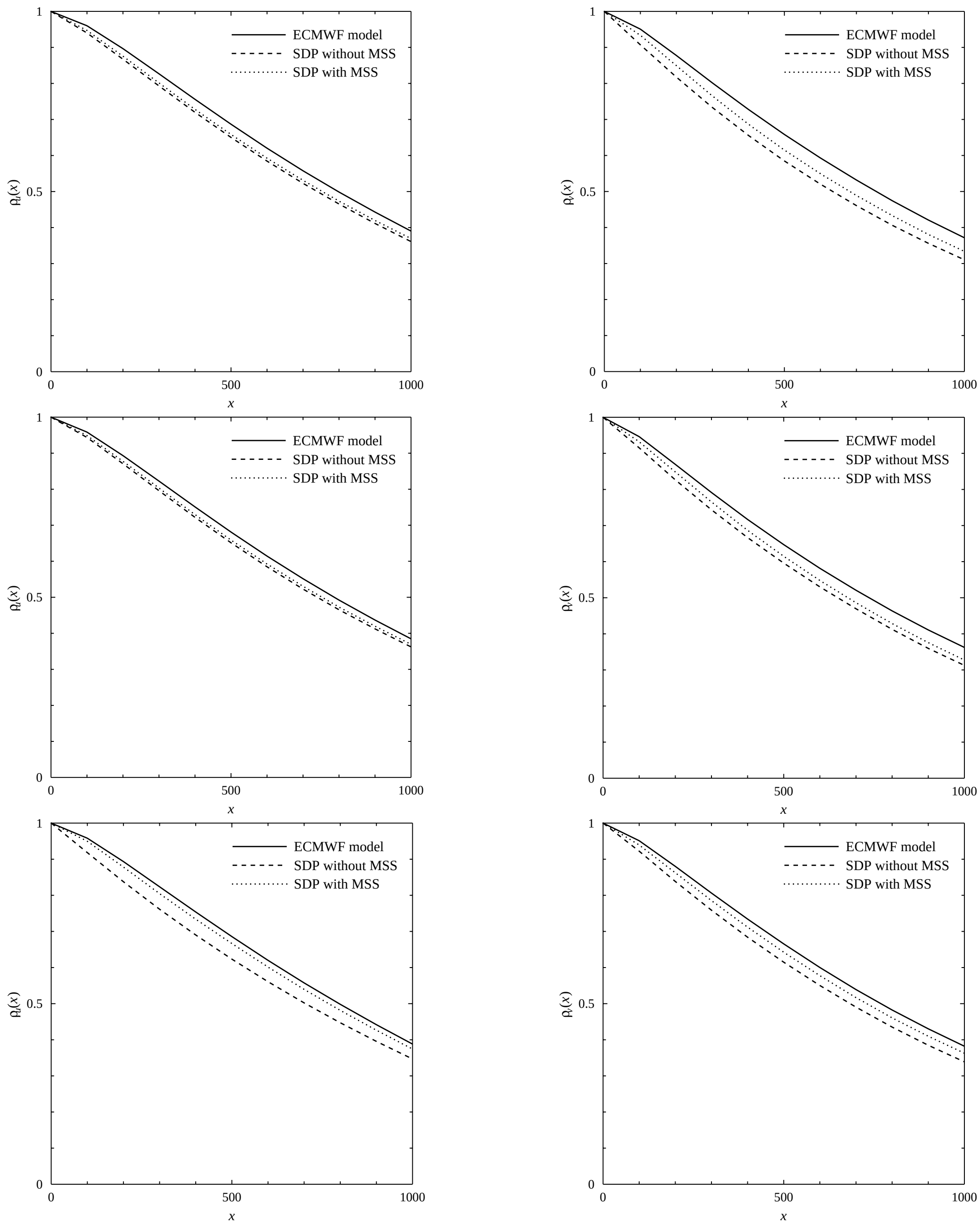

Figure 5.2 Autocorrelation in *u* (left hand panels) and *v* (right hand panels) for the outer swath (top), the sweet swath (middle) and the nadir swath (bottom).

Figure 5.2 shows that the autocorrelation of SDP with or without MSS falls off faster than that of the ECMWF model. This shows that even at 100 km resolution SDP reveals small scale structures in the SeaWinds data that are unresolved in the ECMWF model. The autocorrelation without MSS is slightly higher than that with MSS with the greatest step at 100 km, i.e., at the basic resolution. This indicates that MSS introduces some noise smoothing due to its structure functions. This is strongest in the nadir swath, less strong in the outer swath and relatively weak in the sweet swath, as expected from Figure 4.8 of Vogelzang [2006].

Comment [Ad1]: Dit is de figuur waar je de ruis uitrekent uit de antocovarianties voor diverse processor settings met en zonder MSS

6 Conclusions

In this report two new features of SDP 2.0 are studied: flexible definition of the 2DVAR batch grid size and dimension, and wind retrieval in the outer swath.

It is concluded that for SeaWinds at 25 km resolution the optimal 2DVAR batch grid size is 50 km. This is half of the value used in SDP 1.5 and older versions. The free edge around the observations in the batch grid should be 1800 km. This is much larger than the 500 km employed in SDP 1.5 and earlier. The preferred batch grid dimension is 224 by 240 points (formerly 32 by 32 points). Effects of the batch grid size and dimension show up in areas where observations are sparse, for instance due to extensive rain. The processing time increases because of the larger batch grid, but remains below 5 minutes per orbit on a fast PC.

The quality of the wind vectors in the outer swath is comparable to that in the nadir swath. The standard deviation of the wind vector components *u* and *v* with respect to ECMWF model winds is lowest in the sweet swath and higher in the nadir and outer swaths. When MSS is applied the differences between the various parts of the swath are very small. The MLE and the probability of the selected solution behave similarly for the nadir swath and the outer swath.

The only point of caution in the outer swath results is the fact that the frequency of the KNMI-MLE rain flag setting is significantly lower compared to the sweet and nadir swath. Therefore SDP 2.0 passes too much rain points. This could be cured by lowering the MLE threshold in the KNMI quality control procedure, but at the expense of rejecting many non-raining points. This tuning requires additional information on rain and is outside the scope of this report.

The quality of the 100 km product has been revisited after user requests. Without MSS the SDP 100 km product using NCEP background differs from the ECMWF model by as much as 2 m/s for the zonal component *u* in the nadir swath. Application of the MSS reduces this to 1.4 m/s which is close to the WVC-averaged level of 1.3 m/s.

It is concluded that the wind vectors in the outer swath are useful in SDP-generated wind fields as a stand-alone product. Their quality is comparable to those in the nadir swath. The rain detection is less strict in the outer swath than in the sweet and nadir swath, so assimilation of the outer swath results in NWP models is not recommended. Further it is concluded that the MSS should be switched on in processing SeaWinds data with SDP, also at 100 km resolution.

Comment [Ad2]: Wij hebben eerder SSM/I data gebruikt voor regendetectie. Elke QC is uiteraard een compromis tussen POD en FAR en applicatieafhankelijk. NWP gebruikers willen graag een hoge POD terwijl de weerkamer liever een lage FAR heeft.

Comment [Ad3]: Er is geen enkele gebruiker die over ons produkt heeft geklaagd. Wel is het verzoek binnengekomen om strictere QC dan in de nieuwe NOAA stroom.

References

SCAT group, 2007,
SDP User manual and Reference Guide version 1.5.
Report NWPSAF-KN-UD-002, UKMO, UK.
www.metoffice.gov.uk/research/interproj/nwpsaf/scatterometer/index.html

Vogelzang, J., 2006,
On the quality of high resolution wind fields.
Report NWPSAF-KN-TR-002, UKMO, UK.
www.metoffice.gov.uk/research/interproj/nwpsaf/scatterometer/index.html

Vogelzang, J., 2007,
Validation of 2DVAR on SeaWinds data.
Report NWPSAF-KN-TR-005, UKMO, UK.
www.metoffice.gov.uk/research/interproj/nwpsaf/scatterometer/index.html

Appendix A Software used

Table A.1 shows for each figure of this report the name of the program that generated the data plotted in the figure and the name of the program that made the plot. All programs except PWFX are under control of CVS, so they can always be retrieved if necessary.

Figure	Generating program	Plotting program
2.1 - 2.4	SDP 2.0	PWFX (not in genscat)
4.1 - 4.2	genscat/tools/swat/DSW	genscat/tools/swat/PDN
4.3 - 4.6	genscat/tools/bat/SBA	genscat/tools/bat/SBP
5.1	genscat/tools/swat/DSW	genscat/tools/swat/PDN
5.2	genscat/tools/swat/SAC	genscat/tools/swat/PAC

Table A.1 Generating and plotting programs for the figures in this report.

Appendix B Abbreviations

2DVAR	Two Dimensional Variational Ambiguity Removal
ASCAT	Advanced SCATterometer
ECMWF	European Centre for Medium-Range Weather Forecasts
KNMI	Royal Netherlands Meteorological Institute
MSS	Multiple Solution Scheme
NCEP	National Centers for Environmental Prediction
NOAA	National Oceanic and Atmospheric Administration
NWP	Numerical Weather Prediction
pdf	probability density function
SAF	Satellite Application Facility
SDP	SeaWinds Data Processor
WVC	Wind vector cell